Journal of Advanced Biomedical Sciences
https://jabs.fums.ac.ir/
Online ISSN: 2783-1523
Fasa University of Medical Sciences

Bioinformatics-Based Prediction of Potential Immunogenic Epitopes in *Eimeria tenella* ROP Proteins as Candidate Vaccine Targets

Nastaran Paknejad[1], Ali Dalir Ghaffari[1]✉, Mahdi Khadem Mohammadi[2]

1. Department of Parasitology and Mycology, Faculty of Medicine, Shahed University, Tehran, Iran
2. Student Research Committee, Faculty of Medicine, Shahed University, Tehran, Iran

Article Info

Article Type:
Original Article

Article history:
Received
16 Dec 2025
Received in revised form
31 Jan 2026
Accepted
08 Feb 2026
Published online
10 Mar 2026

Publisher
Fasa University of Medical Sciences

Abstract

Background & Objective: Avian coccidiosis, caused by protozoan parasites of the genus *Eimeria*, imposes substantial economic losses on the global poultry industry. Rhoptry proteins (ROPs), as critical virulence determinants involved in host cell invasion, represent promising targets for vaccine development. This *in silico* study was designed to conduct a comprehensive immunoinformatic characterization of six key *E. tenella* ROPs to identify and prioritize potent T-cell and B-cell epitopes for rational vaccine design.

Materials & Methods: The physicochemical properties, antigenicity, allergenicity, solubility, and post-translational modification (PTM) sites of the six ROPs were systematically predicted using a suite of validated web-based tools. Secondary and tertiary structures were modeled, followed by rigorous refinement and validation procedures. Subsequently, cytotoxic T-lymphocyte (CTL) and helper T-lymphocyte (HTL) epitopes were predicted using human HLA allele surrogates. Their immunogenic potential, including the capacity to induce IFN-γ and IL-4 responses, was thoroughly evaluated. Linear B-cell epitopes were then identified and screened based on antigenicity, non-allergenicity, and optimal solubility profiles.

Results: The findings demonstrated that all selected ROPs are antigenic, non-allergenic, and predominantly hydrophilic, with several exhibiting favorable solubility characteristics. Diverse PTM sites were identified, suggesting complex post-translational regulation. A repertoire of high-affinity and immunogenic CTL and HTL epitopes was detected, among which several candidates showed the potential to induce both IFN-γ (Th1) and IL-4 (Th2) responses, indicative of balanced immune activation. In addition, multiple linear B-cell epitopes with high antigenicity scores were identified.

Conclusion: This study presents the first comprehensive bioinformatic blueprint of six *E. tenella* ROPs and highlights a rich pool of immunogenic epitopes for subsequent experimental validation and vaccine development.

Keywords: *Eimeria tenella,* Rhoptry proteins, Vaccine design, Bioinformatics, *In silico* prediction

Cite this article: Paknejad N, Dalir Ghaffari A, Khadem Mohammadi M. Bioinformatics-Based Prediction of Potential Immunogenic Epitopes in *Eimeria tenella* ROP Proteins as Candidate Vaccine Targets. J Adv Biomed Sci. 2026; 16(2): 191-209.
DOI: 10.18502/jabs.v16i2.20877

Introduction

Avian coccidiosis, an intestinal disease caused by obligate intracellular protozoa of the genus *Eimeria*, remains a persistent threat to poultry health and a major source of economic burden worldwide (1). Global losses attributed to this disease are estimated to exceed US$3 billion annually, underscoring the urgent need for more effective and sustainable control strategies (2). The disease is characterized by

✉ **Corresponding Author: Ali Dalir Ghaffari,** Department of Parasitology and Mycology, Faculty of Medicine, Shahed University, Tehran, Iran.
Email: a.dalirghafari@shahed.ac.ir

severe intestinal lesions, diarrhea, hemorrhagic stools, and impaired weight gain, with *Eimeria tenella* (*E. tenella*) recognized as one of the most pathogenic species due to its high prevalence and pronounced virulence (3). This parasite preferentially infects cecal epithelial cells, resulting in extensive tissue damage and, in severe cases, mortality rates of up to 80% in young chicks (4-7).

Historically, control strategies for coccidiosis have relied heavily on the prophylactic administration of anticoccidial drugs. However, the progressive emergence of drug-resistant *Eimeria* strains, coupled with increasing consumer demand for chemical-free poultry products, has rendered this approach increasingly unsustainable (8). Although live-attenuated vaccines are available, their broader application is constrained by several limitations, including high production costs, complex administration protocols, the potential for reversion to virulence, and the risk of contamination (9). Consequently, the development of next-generation vaccines, particularly recombinant subunit vaccines, has become a critical priority for the sustainable management of coccidiosis (10).

Apicomplexan parasites, including *Eimeria* species, depend on specialized secretory organelles, namely rhoptries (ROPs), micronemes (MICs), and dense granules (GRAs), to release effector proteins that are essential for host cell invasion, formation of the parasitophorous vacuole, and modulation of host cellular processes (11). Among these, ROPs are widely recognized as key virulence factors and potent immunogens. In the closely related parasite *Toxoplasma gondii*, ROPs have been extensively characterized as central mediators of pathogenesis and are known to elicit robust protective immune responses (12). Similarly, ROPs in *E. tenella* play a pivotal role during host cell invasion, and antibodies directed against these proteins have been shown to confer partial protection against infection (13). Proteomic analyses have identified several *E. tenella* ROPs, including EtROP17 and EtROP30, which share homology with *T. gondii* ROPs and are implicated in regulating host cell apoptosis and other pathogenic mechanisms (11).

Despite their recognized functional importance, the immunogenic potential of most *E. tenella* ROPs remains insufficiently characterized. Advances in immunoinformatics provide a powerful, rapid, and cost-effective framework for rational vaccine design, enabling the precise identification of immunodominant epitopes while excluding regions associated with allergenicity or suboptimal immune responses (14). This approach facilitates the development of multi-epitope subunit vaccines with enhanced efficacy and safety profiles. To the best of our knowledge, the present study constitutes the first comprehensive bioinformatic analysis of the biochemical and immunogenic properties of six key *E. tenella* ROPs: ROP17, ROP21, ROP23, ROP25, ROP30, and ROP35. These genes are non-overlapping and located in distinct genomic regions. Collectively, our findings provide a robust foundation for the experimental development of next-generation subunit vaccines targeting this economically significant avian pathogen.

Material and Methods

Protein Sequence Retrieval

The canonical amino acid sequences of six selected *E. tenella* rhoptry proteins (ROPs) were retrieved from the National Center for Biotechnology Information (NCBI) database in FASTA format. The accession numbers used in this study were as follows: XP_013227883.1 (ROP17), XP_013232985.1 (ROP21), XP_013227879.1 (ROP23), XP_013228137.1 (ROP25), XP_013228138.1 (ROP30), and XP_013228816.1 (ROP35). A schematic representation of the *in silico* immunoinformatics workflow employed for the identification of potential vaccine candidates is presented in Figure 1.

Journal of Advanced Biomedical Sciences
Fasa University of Medical Sciences

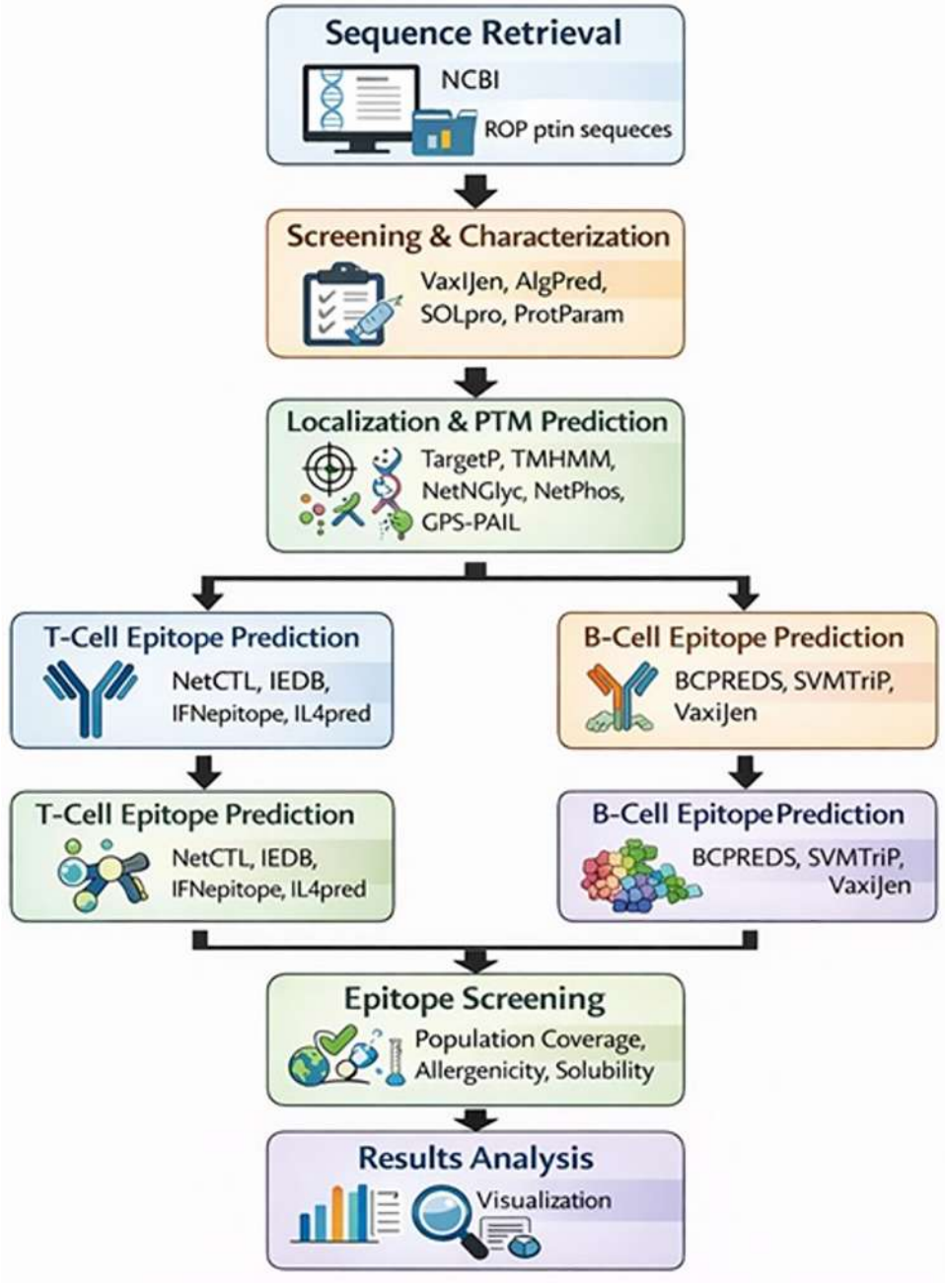

Figure 1. Schematic representation of the *in silico* immunoinformatics workflow used for identifying potential vaccine candidates in this study.

Physicochemical Characterization and Immunological Screening

A preliminary screening of the ROPs was conducted to assess their suitability as vaccine candidates. The antigenicity of each protein was predicted using the VaxiJen v2.0 server (http://www.ddg-pharmfac.net/vaxijen/VaxiJen/VaxiJen.html), employing a threshold of 0.5 for discrimination. This server utilizes an alignment-independent method based on the auto cross covariance (ACC) transformation of protein physicochemical properties (15). Potential allergenicity was evaluated using the AlgPred server (https://webs.iiitd.edu.

in/raghava/algpred/submission.html), which screens for MEME/MAST motifs of known allergens and IgE-specific epitopes (16). The intrinsic solubility of the proteins upon overexpression in *E. coli* was predicted using the SOLpro server (http://scratch.proteomics.ics.uci.edu/), which employs a two-stage support vector machine (SVM) architecture (17).

In addition, key physicochemical parameters were computed using the ExPASy ProtParam tool (18), including molecular weight, theoretical isoelectric point, the number of positively and negatively charged residues, instability index as an indicator of in vitro stability, aliphatic index as a proxy for thermostability, grand average of hydropathicity (GRAVY), and the estimated half-life in mammalian reticulocytes.

Prediction of Subcellular Localization and Transmembrane Topology

To infer the subcellular localization of the ROPs, the TargetP-2.0 server was employed to predict the presence of N-terminal signal peptides that direct proteins into the secretory pathway. In addition, the server distinguishes signal peptides from mitochondrial, chloroplastic, and thylakoid transit peptides (19). Transmembrane helices, which are critical determinants of membrane integration, were predicted using the TMHMM Server v.2.0 with default parameters.

PTM Sites

To elucidate potential functional regulation and structural characteristics, a range of post-translational modification sites was predicted using specialized and validated servers. N-linked glycosylation sites were identified using NetNGlyc 1.0 (20), while O-linked glycosylation sites were predicted using NetOGlyc 4.0 (21). Phosphorylation sites (on Ser, Thr, Tyr) using NetPhos 3.1 (http://www.cbs.dtu.dk/services/NetPhos/) (22), and lysine acetylation sites using GPS-PAIL 2.0 (http://pail.biocuckoo.org/) (23). For the NetNGlyc server, the analysis was configured to scan "all Asn residues" among "all types" for maximum sensitivity, while default parameters were used for other servers.

Secondary and Tertiary Structure Modeling

Secondary structural elements, including α-helices, β-strands, and random coils, were predicted using the Garnier–Osguthorpe–Robson (GOR) IV server (24), which offers an established prediction accuracy of approximately 64.4%. Subsequently, three-dimensional tertiary structures were generated through homology modeling using the automated SWISS-MODEL server (25). For each ROP, the most suitable template was selected from the Protein Data Bank based on optimal sequence identity and query coverage, thereby ensuring high structural reliability.

Refinement and Validation of 3D Protein Structures

To improve the stereochemical and energetic quality of the initial homology models, structural refinement was performed using the GalaxyRefine server. This platform applies molecular dynamics-based simulations to optimize side-chain conformations and overall structural geometry (26). The quality of both the initial and refined models was then rigorously validated through a two-pronged approach. First, the stereochemical integrity was assessed by analyzing the backbone dihedral angles via Ramachandran plots generated within the SWISS-MODEL structure assessment suite (https://swissmodel.expasy.org/assess) (27). Second, the overall model quality was evaluated using the ProSA-web server (https://prosa.services.came.sbg.ac.at/prosa.php), which calculates a Z-score that reflects the deviation of the model's energy profile from that of native proteins of similar size (28).

T-Cell Epitope Prediction Strategy

Given the limited availability of prediction tools specifically trained on avian major histocompatibility complex alleles, a proxy approach based on human leukocyte antigen

supertypes was adopted for both MHC class I and class II epitope prediction (29, 30). This strategy is supported by documented structural similarities and conservation of key peptide anchor residues between chicken MHC haplotypes and their mammalian counterparts, thereby rendering HLA-based predictions informative for avian systems (31).

Cytotoxic T-Lymphocyte (CTL) Epitope Prediction and Immunogenicity Analysis

Potential cytotoxic T-lymphocyte epitopes, defined as 9-mer peptides binding to MHC class I molecules, were predicted using the NetCTL 1.2 server. Predictions were performed across 12 major MHC class I supertypes using a stringent binding affinity threshold of 0.75. To enhance global population relevance, particular emphasis was placed on the A2, A3, and B7 supertypes, which exhibit high prevalence worldwide (32). The immunogenicity of the top predicted binding peptides was then quantitatively scored using the IEDB's dedicated MHC Class I Immunogenicity tool (http://tools.iedb.org/immunogenicity/) to prioritize epitopes most likely to elicit a robust cellular response (33).

Helper T-Lymphocyte (HTL) Epitope Prediction and Functional Characterization

Helper T-lymphocyte (HTL) epitopes (15-mers binding to MHC-II) were predicted using the IEDB MHC-II binding prediction tool (http://tools.iedb.org/mhcii/) against a comprehensive reference set of human HLA-DR, -DP, and -DQ alleles. Epitopes were ranked by a consensus percentile score, where a lower value indicates a higher predicted binding affinity (34). The top-ranking epitopes for each protein were then subjected to a multi-faceted functional characterization. Their antigenicity was scored with VaxiJen v2.0. Their potential to drive specific T-helper cell differentiation was assessed by predicting cytokine induction profiles using two specialized servers: the IFNepitope server (https://webs.iiitd.edu.in/raghava/ifnepitope/predict.php) for interferon-gamma (IFN-γ) induction (a hallmark of Th1 immunity) and the IL4-pred server (https://webs.iiitd.edu.in/raghava/il4pred/design.php) for interleukin-4 (IL-4) induction (a key Th2 cytokine). Finally, the theoretical population coverage of the highest-quality HTL epitopes was calculated using the IEDB Population Coverage tool to estimate their potential efficacy across genetically diverse populations (35).

Linear B-Cell Epitope Prediction and Physicochemical Screening

To identify potential targets for humoral immunity, linear B-cell epitopes were predicted using a dual-server consensus approach to enhance prediction accuracy. The BCPREDS server (http://ailab-projects2.ist.psu.edu/bcpred/index.html), which employs a support vector machine (SVM) with a subsequent kernel (SSK) method, was used with a fixed epitope length of 14 amino acids and a 75% specificity setting (36). Concurrently, the SVMTriP server (http://sysbio.unl.edu/SVMTriP/), which integrates tri-peptide similarity scores with an SVM algorithm, was also used for prediction (37). All epitopes predicted by these servers were then passed through a stringent filtering pipeline to assess their suitability as vaccine components. This included scoring for antigenicity (VaxiJen v2.0), screening for potential allergenicity (AllergenFP v1.0) (38), and evaluating water solubility using the PepCalc online tool (https://pepcalc.com/). Only non-allergenic, highly antigenic, and soluble epitopes were retained as final candidates.

Results

Physicochemical Properties Support Their Viability as Vaccine Candidates

Initial *in silico* screening of the six *E. tenella* rhoptry proteins (ROP17, ROP21, ROP23, ROP25, ROP30, and ROP35) confirmed their favorable characteristics for subunit vaccine development (Table 1).

Table 1. Forecasting antigenicity, allergenicity, common immunological, solubility and physico-chemical characteristics of six E. tenella ROPs proteins.

Parameter	ROP17	ROP21	ROP23	ROP25	ROP30	ROP35
VaxiJen score	0.4924	0.6994	0.5942	0.5572	0.5822	0.6701
AlgPred IgE epitope	-	-	-	-	-	-
MEME/MAST motif	-	-	-	-	-	-
Protein-Sol	0.7148 (Insoluble)	0.9987 (Soluble)	0.7183 (Insoluble)	0.6947 (Insoluble)	0.7430 (Insoluble)	0.8323 (Soluble)
No of AA	665	784	614	671	525	488
Molecular weight	73103	83142	67343	71309	56687	52807
Theoretical pI	8.70	5.82	5.25	8.95	9.30	8.38
Total number of negatively-charged residues (Asp + Glu)	66	75	61	63	53	53
Total number of positively-charged residues (Arg + Lys)	72	64	52	70	65	56
Estimated half-life (h)	30	30	30	30	30	30
Instability index	48.80 (unstable)	64.85 (unstable)	38.75 (stable)	47.62 (unstable)	43.48 (unstable)	47.49 (unstable)
Aliphatic index	87.64	85.29	82.20	93.65	84.23	78.77
Grand average of hydropathicity (GRAVY)	-0.245	-0.283	-0.231	-0.010	-0.237	-0.192

All six proteins were predicted to be non-allergenic by AlgPred 2.0. Antigenicity assessments using VaxiJen v2.0 yielded promising results: five proteins scored above the 0.5 threshold for probable antigens, with only ROP17 slightly below (score: 0.4924).

All candidates exhibited molecular weights well above the 10 kDa threshold generally considered necessary to elicit a robust adaptive immune response. Protein stability was also favorable, as five of the six proteins displayed an instability index below 40, classifying them as stable under in vitro conditions. In parallel, all proteins demonstrated high aliphatic indices, indicative of substantial thermostability. Their negative grand average of hydropathicity values further confirmed their predominantly hydrophilic nature, a characteristic conducive to solubility and effective interaction within aqueous biological environments. Notably, the predicted in vivo half-life in mammalian reticulocytes was consistently long, exceeding 30 hours for all six proteins, thereby suggesting sufficient persistence to facilitate effective immune recognition and activation.

Subcellular Localization and Post-Translational Modifications Indicate Secretory Trafficking and Regulatory Complexity

Subcellular localization predictions were consistent with established rhoptry biology (Table 2). TargetP analysis identified a canonical N-terminal signal peptide in all proteins except ROP23, supporting their targeting to the classical secretory pathway. Complementary TMHMM analysis revealed the presence of a single transmembrane helix in ROP21 and ROP23, suggesting potential membrane association, whereas the remaining proteins are likely to function as soluble secreted effectors.

Post-translational modification profiling revealed a complex and heterogeneous regulatory landscape (Table 3). O-linked glycosylation sites were predicted in all six proteins, while N-linked glycosylation sites were identified in all except ROP35, with ROP23 exhibiting a notably high density of 23 sites. Phosphorylation sites were also extensively predicted across all proteins, with ROP23 and

Table 2. Prediction of signal peptide and transmembrane domains (on the basis of six *E. tenella* ROPs proteins).

Protein name	TargetP Signal peptide prediction			TMHMM Transmembrane domain prediction		
	mTP	SP	Other	ExpAA	First60	PredHel
ROP17	0.0007	0.9462*	0.0531	0.4520	0.38376	0
ROP21	0.0001	0.4606	0.5393	33.252	22.5422	1
ROP23	0.096	0.7485*	0.1555	20.8028	20.7185	1
ROP25	0.0162	0.7569*	0.2269	0.41603	0.01201	0
ROP30	0	0.9997*	0.0003	1.26792	0.0446	0
ROP35	0.0032	0.5561*	0.4407	19.3618	13.0355	0

Table 3. Forecasting of PTM sites of the six *E. tenella* ROPs proteins.

Proteins	No. of N-glycosylation sites	No. of O-glycosylation sites	No. of phosphorylation regions	No. of acetylation regions
ROP17	3	49	64	7
ROP21	2	25	52	1
ROP23	4	13	74	1
ROP25	1	17	40	2
ROP30	2	28	50	14
ROP35	0	20	38	3

Table 4. The assessed secondary structures of *E. tenella* ROPs proteins.

Proteins	Alpha helix (%)	Extended strand (%)	Random coil (%)
ROP17	275 (41.35)	68 (10.23)	322 (48.42)
ROP21	246 (31.38)	74 (9.44)	464 (59.18)
ROP23	186 (30.29)	95 (15.47)	333 (54.23)
ROP25	275 (40.98)	62 (9.24)	334 (49.78)
ROP30	234 (44.57)	61 (11.62)	230 (43.81)
ROP35	175 (35.86)	58 (11.89)	255 (52.25)

ROP17 displaying the highest counts, at 74 and 64 sites, respectively. In addition, lysine acetylation sites were identified in all ROPs, most prominently in ROP30 with 14 sites, and least frequently in ROP21 and ROP23, each containing a single site. Collectively, these findings point to a high degree of post-translational regulation, likely underpinning the functional versatility and stability of these proteins.

Structural Modeling Reveals Intrinsically Disordered Regions and High-Quality 3D Conformations

Secondary structure prediction using the GOR IV algorithm indicated that random coil constitutes the predominant structural element in five of the six proteins, ranging from 48.42% in ROP17 to 59.18% in ROP21 (Figure 2, Table 4). Such elevated coil content is characteristic of intrinsically disordered regions, which are frequently surface-exposed and enriched in immunologically relevant epitopes. In contrast, ROP30 exhibited a distinct structural profile, with α-helices representing the dominant secondary structural element at 44.57%.

High-resolution 3D models were generated via homology modeling and refined to improve structural accuracy (Figure 3).

Ramachandran plot analysis confirmed substantial improvements in stereochemical quality post-refinement: for example, the percentage of residues in the most favored regions rose from 81.15% to 96.38% for ROP17 (Tables 5 and 6, Figure 4).

Journal of Advanced Biomedical Sciences

Fasa University of Medical Sciences

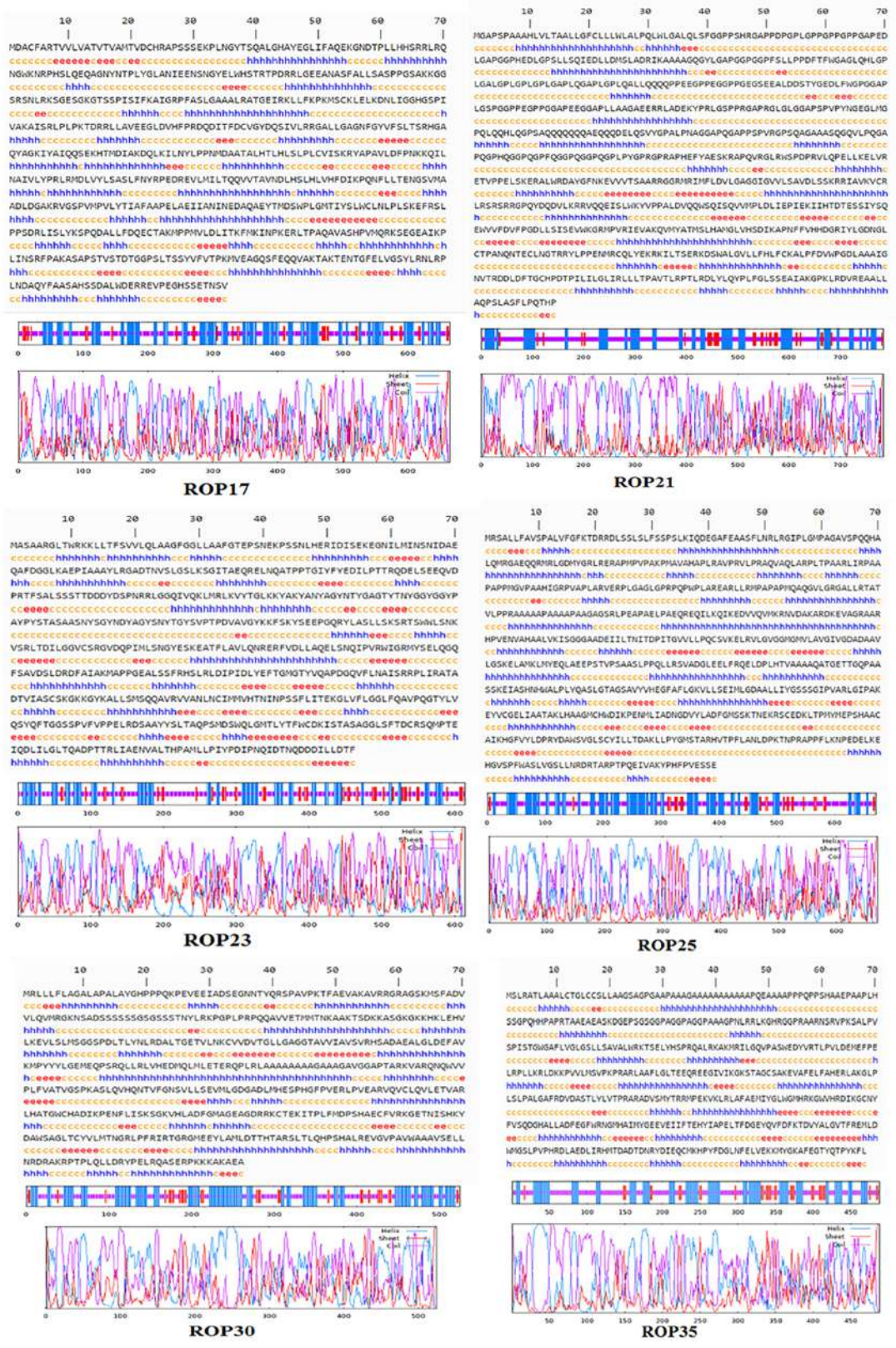

Figure 2. Forecasting secondary structure of *E. tenella* ROPs proteins. Sequences of amino acid colored in blue, yellow, and red show alpha helix, random coil, and extended strand, respectively.

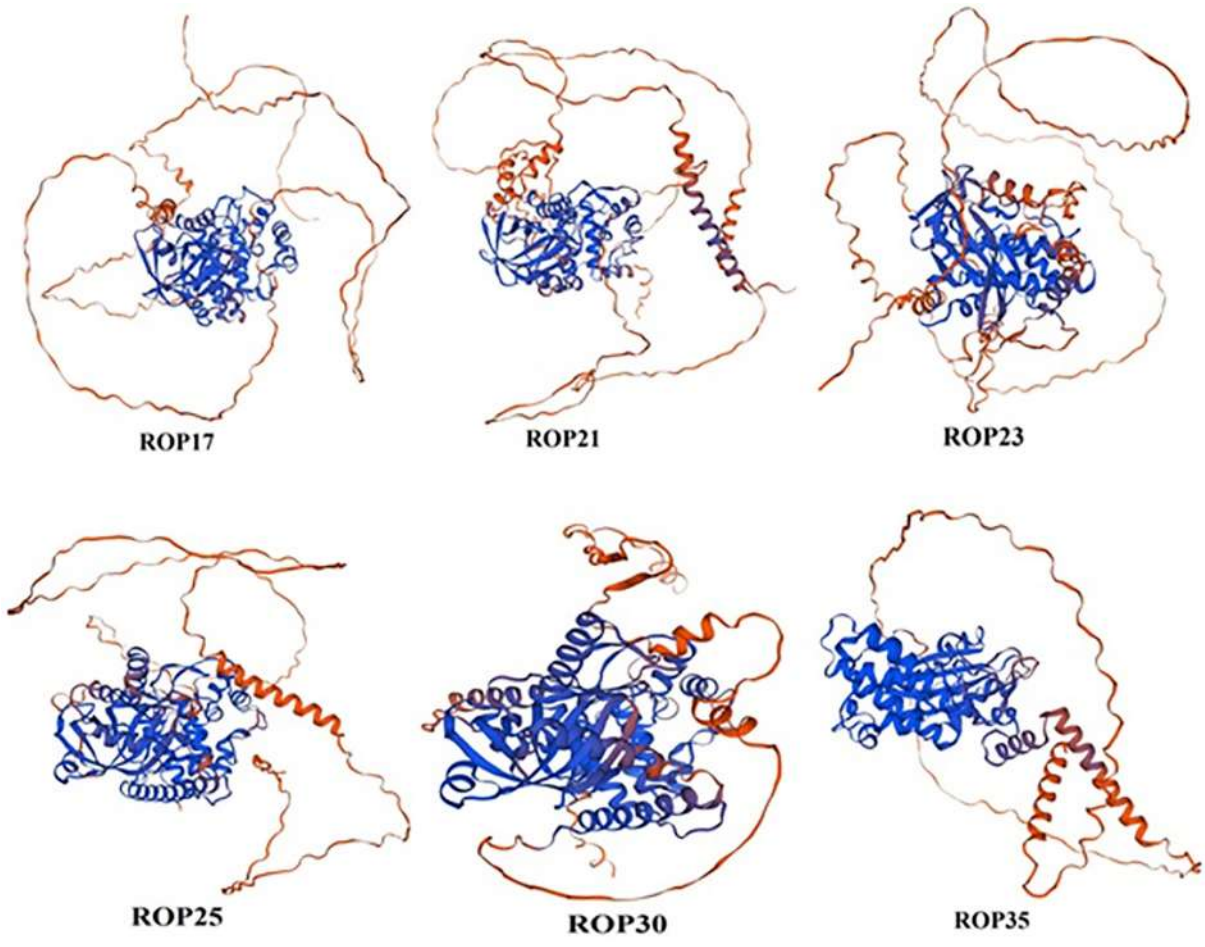

Figure 3. SWISS-MODEL results showing 3D model of each protein with antigenicity.

Table 5. Overall Model Quality

Proteins	Z-Score (before refinement)	Z-Score (after refinement)
ROP17	-7.83	-7.92
ROP21	-8.23	-8.71
ROP23	-4.6	-4.86
ROP25	-8.02	-8.17
ROP30	-9.33	-9.35
ROP35	-8.05	-8.06

Concurrently, ProSA-web Z-scores improved across all models, indicating enhanced overall structural reliability and agreement with experimentally determined protein folds. The final refined structures, summarized in Table 6, exhibited high confidence and were deemed suitable for downstream epitope mapping and structure-guided vaccine design.

Identification of Potent and Immunogenic T- and B-Cell Epitopes

Cytotoxic T-Lymphocyte (CTL) Epitope Candidates

A targeted *in silico* screening approach identified multiple high-affinity 9-mer peptides predicted to bind major histocompatibility complex class I supertypes and to elicit robust immunogenic responses (Table 7).

Table 6. Validation of the 3D structure of *E. tenella* ROPs proteins via Ramachandran plot.

Proteins	Refinement	Ramachandran Favored (%)	Ramachandran Outliers (%)	Rotamer Outliers (%)
ROP17	Before refinement	81.15	9.95	3.93
	After refinement	96.38	0.45	0.18
ROP21	Before refinement	78.90	11.13	4.26
	After refinement	97.31	0.51	0.49
ROP23	Before refinement	81.05	9.80	5.68
	After refinement	97.55	0.65	0.39
ROP25	Before refinement	82.36	11.36	3.10
	After refinement	97.91	0.45	0.78
ROP30	Before refinement	91.01	3.06	0.95
	After refinement	98.85	0.19	0.71
ROP35	Before refinement	89.92	5.76	2.69
	After refinement	98.77	0.00	0.81

Table 7. Forecasting cytotoxic T-lymphocyte epitopes for six *E. tenella* ROPs proteins (the chosen MHC supertypes were A2, A3 and B7).

Protein	CTL Epitopes								
	A2 supertype	Score	Immunogenicity	A3 supertype	Score	Immunogenicity	B7 supertype	Score	Immunogenicity
ROP17	RTVVLVATV	0.7763	0.1387	LLHHSRRLR	1.2359	-0.03213	LVATVTVAM	1.3612	0.1862
	VVLVATVTV	0.9982	0.1701	SLQEQAGNY	0.7956	0.012	APSSSEKPL	1.6542	-0.4755
	ALGHAYEGL	0.9179	0.18247	SASPPGSAK	0.9117	-0.16052	KPLNGYTSQ	0.8497	-0.04449
	HAYEGLIFA	0.8937	0.30283	ASPPGSAKK	0.8000	-0.23047	TPLYGLANI	0.8582	0.04448
ROP21	ALLGFCLLL	1.3941	0.07791	KAAAAGQGY	0.8053	0.04411	APSPAAAHL	1.5827	0.06199
	LLWLALPQL	1.2142	0.01136	RVLQPELLK	1.5082	-0.05255	SPAAAHLVL	1.6287	0.13538
	WLALPQLWL	0.7873	0.00176	LSKERALWR	0.7705	0.23804	LPQLWLGAL	1.6731	0.20796
	QLWLGALQL	0.8838	0.05353	LSAVDLSSK	0.8885	-0. 17088	APGGPHEDL	1.0914	0.16221
ROP23	KLLTFSVVL	1.2785	0.05269	AARGLTWRK	0.7999	0.29382	RGADTNVSL	0.8987	0.00491
	LTFSVVLQL	0.9366	-0.12645	RLGGQIVQK	1.5479	0.02474	LPTTRQDEL	1.4067	0.07024
	LMINSNIDA	0.8498	-0.00522	IVQKLMRLK	1.2609	-0.3935	YPAYPYSTA	1.3564	-0.12224
	YLRGADTNV	0.9315	0.13886	RLKVYTGLK	1.5604	0.0266	YPYSTASAA	1.4827	-0.2098
ROP25	ALLFAVSPA	0.9579	0.04506	SPALVFGFK	0.7536	0.24894	LNRLRGIPL	0.8130	0.19378
	LLFAVSPAL	1.3343	-0.02466	LVFGFKTDR	0.7724	0.02882	RLRGIPLGM	0.8957	0.1805
	RLLRMPAPA	0.7613	-0.10642	SLFSSPSLK	1.7857	-0.44611	MPAGAVSPQ	0.9580	-0.02234
	ALLRTATVL	0.7770	0.17999	RAPMPVPAK	0.8623	-0.13874	AVSPQQHAL	1.0271	-0.23654
ROP30	RLLLFLAGA	0.9621	0.14162	GALAPALAY	0.8603	0.0753	SPAVPKTFA	1.0310	-0.0584
	FLAGALAPA	1.3487	0.101	YQRSPAVPK	0.8620	-0.09528	LPRPQQAVV	1.4151	-0.15906
	AVPKTFAEV	0.7775	0.01892	VVLQVMRGK	1.1091	-0.18178	RPQQAVVET	0.8877	0.01614
	KMSFADVVL	0.9780	0.18204	GSGSSSTNY	0.9030	-0.44332	SPDLTLYNL	0.8653	0.0165
ROP35	STGWGAFLV	0.8756	0.39604	AAAGPNLRR	0.8046	0.05079	GPGAAPAAA	0.9425	0.13391
	FLVGLGSLL	1.1483	-0.0775	AARNSRVPK	0.7649	-0.07373	APAAAGAAA	1.4227	0.17795
	GLGSLLSAV	1.0207	-0.29347	LLSAVALWR	1.3682	0.18276	HAAEPAAPL	1.1051	0.16602
	ALWRKTSEL	1.1452	-0.1306	LSAVALWRK	0.7677	0.29908	APLHSSGPQ	1.0953	-0.26576

Journal of Advanced Biomedical Sciences

Fasa University of Medical Sciences

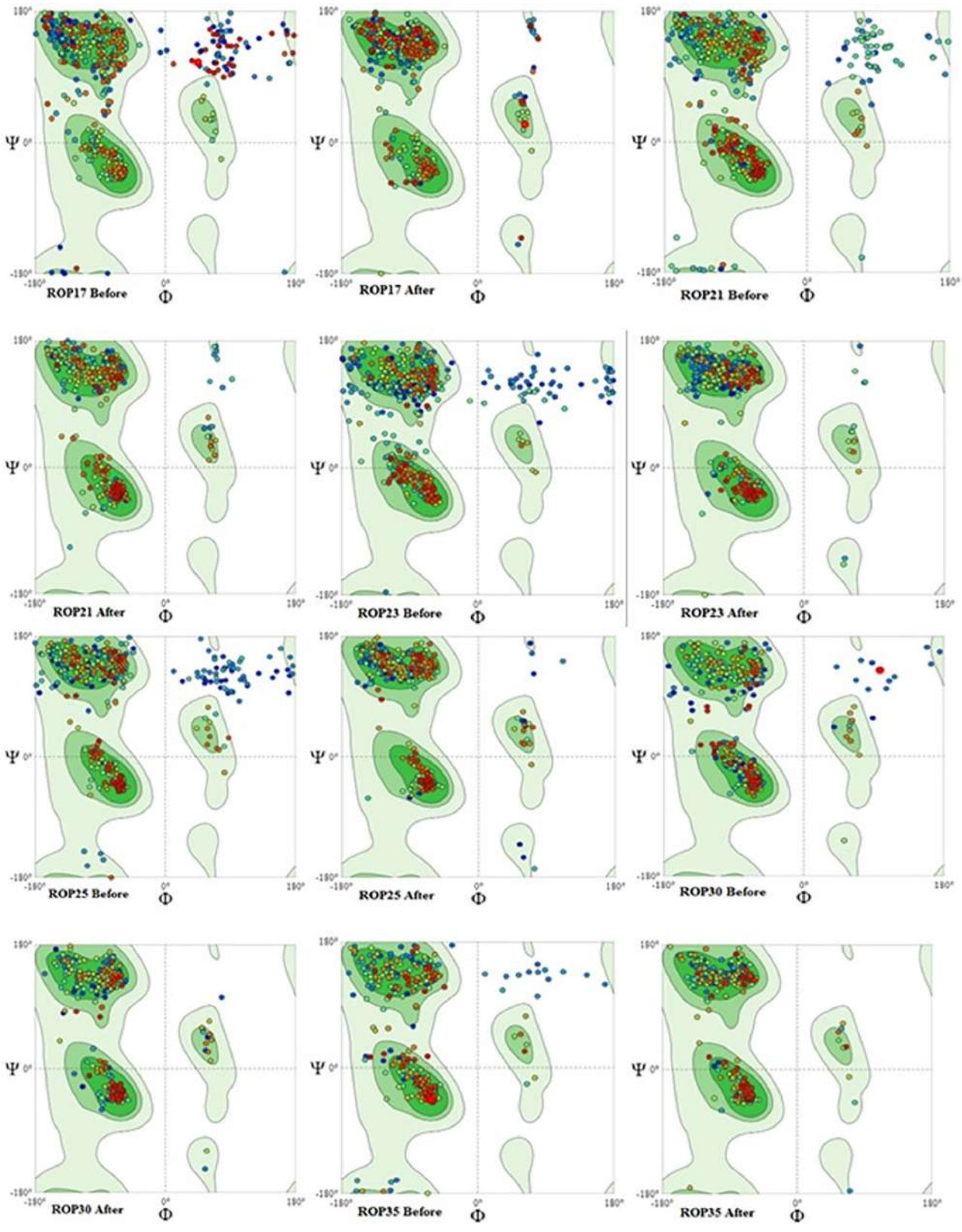

Figure 4. Pictures indicating validation of the 3D structure of *E. tenella* ROPs proteins via Ramachandran plot.

Among these, STGWGAFLV from ROP35 emerged as a leading candidate for the B7 supertype, demonstrating both strong binding affinity (0.8756) and high immunogenicity (0.39604). For the A3 supertype, LSAVALWRK, also derived from ROP35, exhibited strong performance, with a binding score of 0.7677 and an immunogenicity score of 0.29908. The highest predicted binding affinity overall was observed for LPQLWLGAL from ROP21, which achieved a score of 1.6731 and ranked as the top candidate for the A2 supertype, with an associated immunogenicity score of 0.20796. Collectively, these epitopes represent promising targets for the induction of cytotoxic T-cell–mediated immune responses.

Helper T-Lymphocyte (HTL) Epitopes Capable of Inducing Balanced Th1/Th2 Responses

High-affinity 15-mer helper T-lymphocyte epitopes were prioritized based on their antigenicity and cytokine-inducing potential (Table 8). The most antigenic epitope identified was IPVRWIGRMYSELQG from ROP23, with a VaxiJen score of 1.5242, followed by AFLGKVLLSEIMLGD from ROP25 (1.4616) and EEGIVIKGKSTAGCS from ROP35 (1.3792). Importantly, cytokine profiling indicated that these epitopes are capable of supporting a balanced Th1/Th2 immune response. Interferon-gamma–inducing epitopes, indicative of Th1-type immunity, were identified across all six proteins, with ROP30 and ROP35 each containing two such epitopes. In parallel, interleukin-4–inducing epitopes, reflective of Th2 polarization, were also detected. Although no IL-4–inducing epitopes were predicted for ROP21 or ROP25, ROP30 exhibited three top candidates, corresponding to all of its leading epitopes, while ROP23 and ROP35 each harbored two. The co-occurrence of interferon-gamma– and interleukin-4–inducing epitopes within individual ROPs underscores their potential to elicit a comprehensive and balanced adaptive immune response, a highly desirable characteristic in subunit vaccine design.

Highly Antigenic and Soluble Linear B-Cell Epitopes

A consensus-driven prediction pipeline integrating results from two independent servers, followed by stringent filtering for antigenicity, allergenicity, and solubility, yielded a set of high-confidence linear B-cell epitopes (Table 9). At least one 14-mer epitope meeting all selection criteria was identified for each ROP. Among these, two epitopes exhibited exceptionally high predicted antigenicity, namely SADSSSSSSGSGSS from ROP30, with a VaxiJen score of 2.0685, and PEEGPPEGGPPGEG from ROP21, with a score of 1.9330. Additional high-quality candidates included PAKASAPSTVSTDT from ROP17, YESKEATFLAVLQN from ROP23, DPKTNPRAPPFLKN from ROP25, and GLTEEQREEGIVIK from ROP35.

Table 8. Forecasting helper T-lymphocyte specific epitopes for six *E. tenella* ROPs proteins using full HLA reference set of IEDB server.

Protein	Allele	HTL epitope	Method	Percentile rank	Antigenicity	IFN-γ inducing		IL-4 inducing	
						Result	Score	Result	SVM score
ROP17	HLA-DRB1*01:01	AIGRPFASLGAAALR	Consensus (smm/nn/sturniolo)	0.01	-0.0282	Positive	0.4447	Negative	-0.94
	HLA-DRB1*15:06	AIVLYPRLRMDLVYL	Consensus (smm/nn/sturniolo)	0.01	0.9037	Negative	-0.3464	Negative	-0.09
	HLA-DRB1*15:06	ILNAIVLYPRLRMDL	Consensus (smm/nn/sturniolo)	0.01	0.9665	Negative	1	Positive	0.75

Protein	Allele	HTL epitope	Method	Percentile rank	Antigenicity	IFN-γ inducing		IL-4 inducing	
						Result	Score	Result	SVM score
ROP21	HLA-DRB4*01:01	DTPILIL-GLIRLLLT	Consensus (smm/nn/sturniolo)	0.03	0.4055	Negative	32	Negative	-1.16
	HLA-DRB1*11:20	EWVVFDVFP-GDLLSI	Consensus (smm/nn/sturniolo)	0.09	0.2827	Positive	0.1940	Negative	-0.10
	HLA-DRB1*11:04	GGRMRIM-FLDVLGAG	Consensus (smm/nn/sturniolo)	0.23	-0.1813	Negative	-0.5419	Negative	0.16
ROP23	HLA-DRB1*04:23	AAAYLRGAD TNVSLG	Consensus (smm/nn/sturniolo)	0.12	0.6082	Positive	0.4183	Negative	-0.67
	HLA-DRB1*11:04	IPVRWIGRMY SELQG	Consensus (smm/nn/sturniolo)	0.12	1.5242	Negative	-0.2831	Positive	0.29
	HLA-DRB1*04:10	ANLNCIMMV HTNINP	Consensus (smm/nn/sturniolo)	0.13	0.6672	Negative	-1.1226	Positive	0.30
ROP25	HLA-DQA1*05:01/DQB1*03:01	PPRAAAAAPA AAAPA	Consensus (smm/nn/sturniolo)	0.01	0.7453	Negative	1	Negative	0.10
	HLA-DRB1*08:17	AFLGKVLLSE IMLGD	Consensus (smm/nn/sturniolo)	0.25	1.4616	Negative	1	Negative	0.01
	HLA-DQA1*05:01/DQB1*02:01	PQLLRSVADG LEELF	Consensus (smm/nn/sturniolo)	0.25	-0.4892	Positive	0.1364	Negative	0.16
ROP30	HLA-DQA1*05:01/DQB1*03:01	AAAAAAAAG AAAGAV	Consensus (smm/nn/sturniolo)	0.01	0.9223	Positive	1.3706	Positive	0.24
	HLA-DRB1*07:01	DIKPENFLISK SGKV	Consensus (smm/nn/sturniolo)	0.06	0.9383	Negative	1	Positive	1.36
	HLA-DRB1*11:20	FRIRTGRGME EYLAM	Consensus (smm/nn/sturniolo)	0.10	0.1771	Positive	0.0931	Positive	0.25
ROP35	HLA-DQA1*05:01/DQB1*03:01	AAAGAAAA AAAAAAA	Consensus (smm/nn/sturniolo)	0.01	0.8519	Positive	1.5682	Positive	0.27
	HLA-DRB1*08:13	EEGIVIKGK-STAGCS	Consensus (smm/nn/sturniolo)	0.01	1.3792	Negative	1	Negative	0.15
	HLA-DRB1*13:04	EFPELR-PLLKRLDKK	Consensus (smm/nn/sturniolo)	0.07	0.2077	Positive	0.7202	Positive	1.26

Table 9. Forecasting continuous B-cell epitopes of *E. tenella* ROPs proteins using SVMTriP and BCPREDS servers.

Eimeria Markers	Server	Epitope	Score	VaxiJen Score	Allergenicity	Water Solubility
ROP17	BCPred	PAKASAPSTVSTDT	0.99	0.7126	No	Good
		SASPPGSAKKGGSR	0.99	0.6012	No	Good
		DGAKRVGSPVMPVL	0.93	0.1913	No	Good
		TPAQAVASHPVMQR	0.92	0.0808	No	Poor
		NGWKNRPHSLQEQA	0.91	0.3361	No	Good
	SVMTriP	MDLVYLSASLFNYR	1	0.5210	No	Poor
		KHTMDIAKDQLKIL	0.79	0.3317	No	Good
ROP21	BCPred	LGPPGPPGPPGAPE	1	1.3728	Yes	Good
		PGGPPEGPPGGAPE	1	1.3276	Yes	Good
		QGYLGAPGGPGGPF	1	1.4615	No	Poor
		PEEGPPEGGPPGEG	1	1.9330	No	Good
		QGPLPYGPRGPRAP	1	1.0530	Yes	Good
		PNAGGAPQGAPPSP	1	0.7212	Yes	Poor
		GPLGPLGAPLQGAP	1	1.6912	No	Poor
		GGPQGPFQGGPQGG	1	1.1591	No	Poor
		GEDLFWGPGGAPLG	1	-0.2414	Yes	Poor
		GGPPSHRGAPPDPG	1	0.8101	No	Good
		RLGSPPRGAPRGLG	1	0.0036	No	Good
	SVMTriP	VVLSAVDLSSKRRI	1	-0.1397	No	Good
		SQIEDLLDMSLADR	0.84	-0.0410	Yes	Good
ROP23	BCPred	EQRELNQATPPTGI	0.99	0.4407	No	Good
		FAIAKMAPPGEALS	0.98	0.7076	No	Poor
		NYTGYSVPTPDVAV	0.98	0.7317	No	Poor
		TGGSSPVFVPPELR	0.97	0.6111	No	Good
		IASCSKGKKGYKAL	0.96	0.4692	No	Good
		IPNQIDTNQDDDIL	0.96	0.5550	No	Good
		ILGLTQADPTTRLI	0.94	0.5120	No	Poor
		GMGTYVQAPDGQVF	0.91	0.8828	No	Poor
	SVMTriP	YESKEATFLAVLQN	1	0.6337	No	Good
		SSFLITEKGLVFLG	0.89	0.1942	No	Poor
		RIDISEKEGNILMI	0.81	0.0445	No	Good
ROP25	BCPred	RPAAPAPPMGVPAA	1	0.6689	Yes	Poor
		AAAPAAAAPAAGAG	1	0.6241	Yes	Poor
		NRDRTARPTPQEIV	1	0.7807	No	Good
		GIPLGMPAGAVSPQ	0.99	0.6490	Yes	Poor
		DPKTNPRAPPFLKN	0.99	0.8878	No	Good
		RERAPMPVPAKPMA	0.99	0.4945	No	Good
		MPAPAPMQAQGVLG	0.99	0.8132	No	Poor
		PEAPAELPAEQREQ	0.99	0.6666	Yes	Good
		ATGETTGQPAASSK	0.99	0.8609	No	Good
	SVMTriP	LLSEIMLGDAALLI	1	0.8250	No	Poor
		LLRSVADGLEELFR	0.86	-0.5213	Yes	Good

Eimeria Markers	Server	Epitope	Score	VaxiJen Score	Allergenicity	Water Solubility
ROP30	BCPred	AAGAVGGAPTARKV	1	0.6788	No	Good
		SADSSSSSSGSGSS	1	2.0685	No	Good
		DKKASGKGKKHKLE	0.99	1.4135	No	Good
		QASERPKKKAKAEA	0.99	1.3174	No	Good
		PALAYGHPPPQKPE	0.99	0.5034	No	Good
		RKPGPLPRPQQAVV	0.99	0.0519	Yes	Good
		GEAGDRRKCTEKIT	0.99	1.1205	No	Good
		SEGNNTYQRSPAVP	0.98	0.4451	No	Good
		RDRAKRPTPLQLLD	0.97	0.7638	No	Good
		MQLMLETERQPLRL	0.96	0.7496	No	Good
	SVMTriP	TVFGNSVLLSEVML	1	1.3288	No	Poor
		YNLRDALTGETVLN	0.84	0.5214	No	Good
ROP35	BCPred	PAGGPAGGPAAAGP	1	1.4864	Yes	Poor
		APQEAAAAPPPQPP	1	0.6379	No	Good
		GSAGPGAAPAAAGA	1	1.1935	No	Poor
		GHRGGPRAARNSRV	1	0.6656	No	Good
		GPQHHPAPRTAAEA	0.99	0.2364	Yes	Good
		GLTEEQREEGIVIK	0.97	1.2915	No	Good
		PALGAFRDVDASTL	0.92	0.0879	No	Good
		KPVVLMSVPKPRAR	0.92	0.8301	No	Good
		EYQVFDFKTDVYAL	0.92	0.9458	Yes	Good
	SVMTriP	EVAFELFAHERLAK	1	0.6987	Yes	Good
		AFRDVDASTLYLVT	0.86	-0.1757	No	Poor
		SLLSAVALWRKTSE	0.80	-0.4474	No	Good

All selected epitopes were predicted to be non-allergenic, highly soluble, and surface-accessible, which are essential attributes for effective B-cell recognition and antibody production. These peptides therefore constitute promising targets for the induction of strong and durable humoral immune responses.

Discussion

The escalating emergence of drug-resistant *Eimeria* strains, together with the practical and safety limitations associated with currently available live-attenuated vaccines, underscores the urgent need for next-generation immunoprophylactic strategies against avian coccidiosis. Recombinant subunit vaccines, designed around well-defined and highly immunogenic antigens, represent a promising approach that effectively balances efficacy, safety, scalability, and cost-effectiveness (11). Rhoptry proteins, which play central roles in host cell invasion, parasitophorous vacuole formation, and immune modulation, constitute an attractive reservoir of vaccine targets owing to their surface exposure, evolutionary conservation, and established involvement in parasite pathogenesis (39, 40). To the best of our knowledge, the present study provides the first comprehensive *in silico* characterization of six relatively understudied *E. tenella* ROPs, namely ROP17, ROP21, ROP23, ROP25, ROP30, and ROP35, and offers a multidimensional framework encompassing their physicochemical, structural, and immunogenic attributes to guide rational subunit vaccine design. Initial bioinformatic screening confirmed the fundamental suitability of these ROPs as vaccine candidates. All six proteins were predicted to be non-allergenic, satisfying a critical safety requirement for both clinical and

veterinary applications (41). With the exception of ROP17, which exhibited a VaxiJen score of 0.4924, all proteins demonstrated strong antigenicity exceeding the 0.5 threshold, and each possessed a molecular weight well above the minimum threshold generally required for effective immunogenicity. Their negative grand average of hydropathicity values indicate a predominantly hydrophilic nature, which is favorable for solubility and handling in aqueous environments, whereas their high aliphatic indices suggest substantial thermostability. Both features are advantageous for recombinant protein expression and downstream formulation. Subcellular localization analysis further supports their biological relevance, as five of the six ROPs were predicted to contain N-terminal signal peptides, consistent with secretion via the classical secretory pathway and subsequent interaction with host cells.

Moreover, the identification of diverse and abundant post-translational modification sites, including numerous N-linked and O-linked glycosylation motifs as well as extensive phosphorylation sites, indicates a high degree of regulatory complexity governing their native function. Although such modifications are likely essential for parasite fitness, their absence in prokaryotic expression systems such as *Escherichia coli* may, in fact, prove advantageous for vaccine development. Specifically, the lack of post-translational modifications could facilitate the exposure of otherwise cryptic epitopes while simplifying large-scale production, without necessarily compromising immunogenicity.

A defining characteristic of effective vaccines is their capacity to elicit both humoral and cellular immune responses. In this regard, the present epitope mapping analysis revealed a rich and complementary repertoire of B-cell and T-cell targets. The identification of highly antigenic and soluble linear B-cell epitopes, particularly SADSSSSSSGSGSS derived from ROP30 and PEEGPPEGGPPGEG from ROP21, highlights promising candidates for the induction of neutralizing antibodies. This observation is further supported by structural predictions demonstrating that most ROPs are enriched in random coil regions, which are typically associated with intrinsically disordered and surface-exposed segments that are readily accessible to B-cell receptors.

Equally important, the analysis identified T-cell epitopes capable of inducing a balanced Th1/Th2 immune response, a key determinant of protective immunity against intracellular pathogens. The presence of multiple interferon-gamma–inducing helper T-lymphocyte epitopes, together with high-affinity cytotoxic T-lymphocyte epitopes targeting major MHC class I supertypes such as A2, A3, and B7, indicates a strong potential for activating cellular immune mechanisms required for parasite clearance. Concurrently, the prediction of interleukin-4–inducing helper T-cell epitopes in ROP23, ROP30, and ROP35 suggests a complementary Th2 response that would promote B-cell activation and antibody production. This dual immunological capacity aligns closely with the profile of highly efficacious vaccines and strongly supports the incorporation of these ROPs, or their immunodominant regions, into a multi-epitope vaccine construct (42, 43). Such a strategy would enable the selective inclusion of protective epitopes while minimizing non-protective or potentially immunosuppressive regions.

Limitations

Despite the robustness of the computational framework employed, several inherent limitations of *in silico* prediction must be acknowledged. Although the analytical pipeline incorporated well-validated algorithms, all findings require empirical validation in avian experimental models. In particular, the use of human leukocyte antigen alleles as surrogates

for the chicken major histocompatibility complex B-locus represents a pragmatic yet imperfect approximation, necessitated by the limited availability of validated avian-specific prediction tools. Consequently, these predictions may not fully capture the nuances of antigen presentation in the avian immune system. In addition, the present study focused exclusively on linear B-cell epitopes, whereas conformational epitopes, which frequently dominate antibody responses to native proteins, were not assessed. Finally, the functional implications of the predicted post-translational modifications in terms of antigen processing, presentation, and immunogenicity remain to be experimentally determined. Notwithstanding these limitations, the present study provides a rigorously prioritized and evidence-based portfolio of ROP-derived epitopes and full-length protein candidates that can substantially accelerate downstream experimental investigations, including recombinant protein production, immunogenicity assessment, and protective efficacy studies in poultry.

Conclusion

This comprehensive immunoinformatic investigation systematically delineates the antigenic landscape of six key *E. tenella* rhoptry proteins, namely ROP17, ROP21, ROP23, ROP25, ROP30, and ROP35. A robust set of non-allergenic and highly antigenic B-cell and T-cell epitopes was identified and prioritized, with strong potential to elicit a balanced Th1/Th2 immune response, which is essential for effective protection against intracellular apicomplexan parasites. Supported by favorable physicochemical properties, reliable structural features, and compelling immunological profiles, these epitopes provide a rational and data-driven foundation for the development of a next-generation multi-epitope subunit vaccine against avian coccidiosis. Given the substantial economic burden imposed by this disease on the global poultry industry, together with the increasing challenges of drug resistance and the limitations of existing live vaccines, such a targeted vaccine strategy represents a promising avenue toward sustainable, safe, and scalable disease control. The candidates identified herein warrant prompt experimental validation through in vitro immunogenicity assays and in vivo challenge studies in avian models, thereby facilitating the translation of these computational insights into a practical and effective veterinary intervention.

Acknowledgments

The authors gratefully acknowledge their colleagues at Shahed University for their valuable feedback and constructive discussions, which contributed significantly to the improvement of this manuscript.

Conflict of Interest

The authors declare that there is no conflict of interest.

Availability of Data and Materials

All data generated or analysed during this study are included in this published article.

Abbreviations

3D, three-dimensional; ANN, artificial neural network; CD, cluster of differentiation; CTL, cytotoxic T lymphocyte; GRA, dense granule antigen; GRAVY, grand average of hydropathicity; IC_{50}, half maximal inhibitory concentration; IEDB, immune epitope database; IFN-γ, interferon-γ; IgE, immunoglobulin E; IgG, immunoglobulin G; MHC, major histocompatibility complex; MIC, microneme protein; MQ, macrophage; MW, molecular weight; NK, natural killer cell; PDB, protein data bank; pI, isoelectric point; PTM, post-translational modification; ROP, rhoptry protein; SAG, surface antigen; SVM, support vector machine; *T. gondii*, *Toxoplasma gondii*; TH, T-helper cell.

Code of Ethics

IR.SHAHED.REC.1402.138

Authors' Contributions

N. Paknejad, A. Dalir Ghaffari, and M. Khadem Mohammadi conceived and designed the study protocol. A. Dalir Ghaffari supervised the research. N. Paknejad, A. Dalir Ghaffari, and M. Khadem Mohammadi performed the bioinformatics analyses. A. Dalir Ghaffari and M. Khadem Mohammadi drafted the manuscript. All authors critically reviewed and approved the final version of the manuscript.

References

1 Brown Jordan A, Blake D, Beard J, Beharry A, Serrette L, Soleyn A, et al. Molecular identification of Eimeria species in broiler chickens in Trinidad, West Indies. Vet Sci. 2018;5(1):12.
2 Cheng P, Wang C, Lin X, Zhang L, Fei C, Zhang K, et al. Pharmacokinetics of a novel triazine ethanamizuril in rats and broiler chickens. Res Vet Sci. 2018;117:99-103.
3 Zhang X, Li S, Zheng M, Zhang L, Bai R, Li R, et al. Effects of the PI3K/Akt signaling pathway on the apoptosis of early host cells infected with Eimeria tenella. Parasitol Res. 2020;119(8):2549-61.
4 Bussière FI, Niepceron A, Sausset A, Esnault E, Silvestre A, Walker RA, et al. Establishment of an in vitro chicken epithelial cell line model to investigate Eimeria tenella gamete development. Parasit Vectors. 2018;11:1-8.
5 Xu Z, Zheng M, Zhang L, Zhang X, Zhang Y, Cui X, et al. Effect of ATP and Bax on the apoptosis of Eimeria tenella host cells. BMC Vet Res. 2017;13(1):1-9.
6 Xu Z-y, Zheng M-x, Zhang L, Gong X, Xi R, Cui X-z, et al. Dynamic expression of death receptor adapter proteins tradd and fadd in Eimeria tenella-induced host cell apoptosis. Poult Sci 2017;96(5):1438-44.
7 Li S, Zheng M-x, Xu H-c, Cui X-z, Zhang Y, Zhang L, et al. Mitochondrial pathways are involved in Eimeria tenella-induced apoptosis of chick embryo cecal epithelial cells. Parasitol Res. 2017;116:225-35.
8 Blake DP, Knox J, Dehaeck B, Huntington B, Rathinam T, Ravipati V, et al. Re-calculating the cost of coccidiosis in chickens. Vet Res. 2020;51:1-14.
9 Jenkins MC, Parker C, Ritter D. Eimeria oocyst concentrations and species composition in litter from commercial broiler farms during anticoccidial drug or live Eimeria oocyst vaccine control programs. Avian Dis. 2017;61(2):214-20.
10 Lee Y, Lu M, Lillehoj HS. Coccidiosis: recent progress in host immunity and alternatives to antibiotic strategies. Vaccines. 2022;10(2):215.
11 Foroutan M, Ghaffari AD, Soltani S, Majidiani H, Taghipour A, Sabaghan M. Bioinformatics analysis of calcium-dependent protein kinase 4 (CDPK4) as Toxoplasma gondii vaccine target. BMC Res Notes. 2021;14(1):50.
12 Possenti A, Di Cristina M, Nicastro C, Lunghi M, Messina V, Piro F, et al. Functional characterization of the thrombospondin-related paralogous proteins rhoptry discharge factors 1 and 2 unveils phenotypic plasticity in Toxoplasma gondii rhoptry exocytosis. Front Microbiol. 2022;13:899243.
13 Bermúdez M, Arévalo-Pinzón G, Rubio L, Chaloin O, Muller S, Curtidor H, et al. Receptor–ligand and parasite protein–protein interactions in Plasmodium vivax: analysing rhoptry neck proteins 2 and 4. Cell Microbiol. 2018;20(7):e12835.
14 Asghari A, Shamsinia S, Nourmohammadi H, Majidiani H, Fatollahzadeh M, Nemati T, et al. Development of a chimeric vaccine candidate based on Toxoplasma gondii major surface antigen 1 and apicoplast proteins using comprehensive immunoinformatics approaches. EUR J PHARM SCI. 2021;162:105837.
15 Majid M, Andleeb S. Designing a multi-epitopic vaccine against the enterotoxigenic Bacteroides fragilis based on immunoinformatics approach. Sci Rep. 2019;9(1):19780.
16 Sharma N, Patiyal S, Dhall A, Pande A, Arora C, Raghava GP. AlgPred 2.0: an improved method for predicting allergenic proteins and mapping of IgE epitopes. Brief Bioinform. 2021;22(4):bbaa294.
17 Magnan CN, Randall A, Baldi P. SOLpro: accurate sequence-based prediction of protein solubility. Bioinform. 2009;25(17):2200-7.
18 Taghipour A, Tavakoli S, Sabaghan M, Foroutan M, Majidiani H, Soltani S, et al. Immunoinformatic Analysis of Calcium-Dependent Protein Kinase 7 (CDPK7) Showed Potential Targets for Toxoplasma gondii Vaccine. J Parasitol Res. 2021;2021(1):9974509.
19 Armenteros JJA, Salvatore M, Emanuelsson O, Winther O, Von Heijne G, Elofsson A, et al. Detecting sequence signals in targeting peptides using deep learning. Life Sci Alliance. 2019;2(5).
20 Gupta R, Jung E, Brunak S. Prediction of N-glycosylation sites in human proteins http://www. cbs.

dtu. dk/services. NetNG lyc. 2004.
21 Steentoft C, Vakhrushev SY, Joshi HJ, Kong Y, Vester-Christensen MB, Schjoldager KTB, et al. Precision mapping of the human O-GalNAc glycoproteome through SimpleCell technology. EMBO J. 2013;32(10):1478-88.
22 Blom N, Gammeltoft S, Brunak S. Sequence and structure-based prediction of eukaryotic protein phosphorylation sites. J Mol Biol. 1999;294(5):1351-62.
23 Deng W, Wang C, Zhang Y, Xu Y, Zhang S, Liu Z, et al. GPS-PAIL: prediction of lysine acetyltransferase-specific modification sites from protein sequences. Sci Rep. 2016;6(1):39787.
24 Ghaffari AD, Rahimi F. Immunoinformatics studies and design of a novel multi-epitope peptide vaccine against Toxoplasma Gondii based on calcium-dependent protein kinases antigens through an in-silico analysis. Clin Exp Vaccine Res. 2024;13(2):146.
25 Guex N, Peitsch MC, Schwede T. Automated comparative protein structure modeling with SWISS-MODEL and Swiss-PdbViewer: A historical perspective. Electrophoresis. 2009;30(S1):S162-S73.
26 Park H, Seok C. Refinement of unreliable local regions in template-based protein models. Proteins:Struct Funct Bioinf. 2012;80(8):1974-86.
27 Bertoni M, Kiefer F, Biasini M, Bordoli L, Schwede T. Modeling protein quaternary structure of homo- and hetero-oligomers beyond binary interactions by homology. Sci Rep. 2017;7(1):10480.
28 Wiederstein M, Sippl MJ. ProSA-web: interactive web service for the recognition of errors in three-dimensional structures of proteins. Nucleic Acids Res. 2007;35(suppl_2):W407-W10.
29 Mugunthan SP, Harish MC. Multi-epitope-based vaccine designed by targeting cytoadherence proteins of Mycoplasma gallisepticum. ACS omega. 2021;6(21):13742-55.
30 Omony JB, Wanyana A, Mugimba KK, Kirunda H, Nakavuma JL, Otim-Onapa M, et al. Epitope peptide-based predication and other functional regions of antigenic F and HN proteins of waterfowl and poultry avian avulavirus serotype-1 isolates from Uganda. Front vet sci. 2021;8:610375.
31 Tan L, Liao Y, Fan J, Zhang Y, Mao X, Sun Y, et al. Prediction and identification of novel IBV S1 protein derived CTL epitopes in chicken. Vaccine. 2016;34(3):380-6.
32 Larsen MV, Lundegaard C, Lamberth K, Buus S, Lund O, Nielsen M. Large-scale validation of methods for cytotoxic T-lymphocyte epitope prediction. BMC bioinformatics. 2007;8:1-12.
33 Calis JJ, Maybeno M, Greenbaum JA, Weiskopf D, De Silva AD, Sette A, et al. Properties of MHC class I presented peptides that enhance immunogenicity. PLoS Comput Biol. 2013;9(10):e1003266.
34 Vita R, Mahajan S, Overton JA, Dhanda SK, Martini S, Cantrell JR, et al. The immune epitope database (IEDB): 2018 update. Nucleic Acids Res. 2019;47(D1):D339-D43.
35 Bui H-H, Sidney J, Dinh K, Southwood S, Newman MJ, Sette A. Predicting population coverage of T-cell epitope-based diagnostics and vaccines. BMC bioinformatics. 2006;7(1):1-5.
36 Foroutan M, Karimipour-Saryazdi A, Ghaffari AD, Majidiani H, Arzani Birgani A, Karimzadeh-Soureshjani E, et al. In Silico Analysis and Characterization of the Immunogenicity of Toxoplasma gondii Rhoptry Protein 18. Bioinformatics biol insights. 2025;19:11779322251315924.
37 Yao B, Zhang L, Liang S, Zhang C (2012) SVMTriP: A Method to Predict Antigenic Epitopes Using Support Vector Machine to Integrate Tri-Peptide Similarity and Propensity. PLoS ONE 7(9): e45152.
38 Dimitrov I, Naneva L, Doytchinova I, Bangov I. AllergenFP: allergenicity prediction by descriptor fingerprints. Bioinformatics. 2014;30(6):846-51.
39 Lebrun M, Carruthers VB, Cesbron-Delauw M-F. Toxoplasma secretory proteins and their roles in cell invasion and intracellular survival. Toxoplasma gondii: Elsevier; 2014. p. 389-453.
40 Meng Y-J, Mu B-J, Liu X-X, Yu L-M, Zheng W-B, Xie S-C, et al. Transcriptional changes in LMH cells induced by Eimeria tenella rhoptry kinase family protein 17. Front vet sci. 2022;9:956040.
41 Shams M, Javanmardi E, Nosrati MC, Ghasemi E, Shamsinia S, Yousefi A, et al. Bioinformatics features and immunogenic epitopes of Echinococcus granulosus Myophilin as a promising target for vaccination against cystic echinococcosis. Infect Genet Evol. 2021;89:104714.
42 Pandey RK, Bhatt TK, Prajapati VK. Novel immunoinformatics approaches to design multi-epitope subunit vaccine for malaria by investigating anopheles salivary protein. Sci Rep. 2018;8(1):1125.
43 Dar HA, Zaheer T, Shehroz M, Ullah N, Naz K, Muhammad SA, et al. Immunoinformatics-aided design and evaluation of a potential multi-epitope vaccine against Klebsiella pneumoniae. Vaccines. 2019;7(3):88.